Supplemental Information

During model refinement for the ApG^o structure, we observed density corresponding to a second alternative conformation of the phosphate backbone between the oxoG and the 5'-A. We chose to treat the two conformations as two separate structures, referring to them as conformation 1 and conformation 2. Interestingly, alignments of the ApG^o backbone with other members of the set show that conformation 1 overlays well with the GpG^o state, whereas conformation 2 overlays well with the TpG^o and CpG^o states (Fig. S4). The GpG^o and ApG^o conformation 1 structures are the most underwound compared to the other members of the set, resulting in the 5' base fully stacking with the oxoG. In order to maintain consistency with our previous analysis, we chose the GpG^o structure as the reference structure for the displacement measurements.

Shown in Fig. S3, both ApG^o conformations show minimal displacement of the 5'-base from the GpG^o state, while the 5'-pyrimidine in the CpG^o structure shows a 1.0 Å displacement in the direction of the major groove. To our surprise, the TpG^o structure had a net displacement of only 0.1 Å; however, analysis of the base-step parameters indicates that TpG^o structure has a significantly larger Roll angle compared to other members of the set (29° compared to 6-15°; Fig. S5). Roll is defined as the degree of opening between the two planes formed by each base pair step. An increase in Roll angle causes the 5'-base to angle away from the oxoG, increasing the distance between the two bases. Since the π-π interactions important for the aromatic contribution to base stacking are distance dependent, any increase in distance between the two bases has the potential to weaken stacking interactions.

The influence of sequence at the 5'-position on potential stacking interactions between the 5'-base and the oxoG remains evident in this second set of NpG^o structures. Consistent with our previous observations, structures with a 5'-pyrimidine have less favorable stacking arrangements, due to either a reduction in the overlap between the 5' base and the oxoG as a result of translational motion in the direction of the minor groove or an increase in distance between the two bases as a result of changes in the Roll angle. In contrast, structures with a 5'-purine remain stacked to the oxoG. This second set of structures confirms that our previous observations are independent of crosslinking position, and are determined solely by the identity of the base 5' to the oxoG.

SUPPLEMENTARY FIGURE CAPTIONS

Figure S1. (**A**) Comparison of NpG^o backbone conformations for the oxoG-containing and opposing strands. Phosphate groups are shown as spheres. The phosphate group between the oxoG and its 5'-stacking neighbor, and the corresponding phosphate on the opposing strand, is colored in red. Double-headed arrow indicates movement in phosphate position. (**B**) Crystal contacts between symmetry mates. Overlay of all NpG^o DNA chains with the protein portion from TpG^o. **(C)** Alignment of all NpGo (left) and NpG (right) structures showing movement of base N within each set.

Figure S2. Electron density for the (**A**) GpG^o, (**B**) TpG^o, and (**C**) ApG^o structures. The alignments are the same as in Fig. 4, with the GpG^o structure aligned to the previously published CpG^o structure (3GP1), shown in blue, while the other NpG^o structures are aligned with the GpG^o structure from this set (gray). Electron density for the GpG^o and TpG^o/ ApG^o structures clearly shows a distinct shift in the position of each 5'-base relative to the CpG^o and GpG^o states, respectively. The Fo-Fc maps are contoured to 1.5 σ.

Figure S3. Superposition of NpG^o structures with GpG^o from structures crosslinked to an alternative phosphate position (set 2). The white circles mark the glycosidic nitrogen on the 5'-stacking neighbor. (**A**) CpG^o; (**B**) TpG^o; (**C**) ApG^o. The distances between glycosidic nitrogens measured for each pair are shown in (**D**). The net displacement of the 5'-base is calculated by subtracting the movement of oxoG (pink bars) from the movement of the 5' base (dark blue bars).

Figure S4. Alternative backbone conformation seen for ApG^o crosslinked using a different phosphate group. (**A**) Alternative conformations 1 and 2. The view is towards the oxoG-containing strand. The overlay shows electron density for two phosphate positions, using the 2Fo-Fc map contoured at 1.0 σ. (**B**) Alignment with CpG^o; (**C**) Alignment with TpG^o; (**D**) Alignment with GpG^o.

Figure S5. Effect of Roll angle on base-stacking. The target base-pair is shown in dark gray, the 5'-base-pair shown in light gray. Gray rectangles indicate the plane of each base pair; dotted arrows represent the position of each plane relative to each other. The angles correspond to Roll values for that base step as calculated by 3DNA. A table with Roll angles for each NpGo structure in the second set is shown to the right.

Figure S6. Hydrogen bonding distances between the target base and the opposing base for each NpG (lefthand column) and NpG^o. structure (righthand column). The target G is colored in blue, the target oxoG is colored in red, and the opposing bases are colored orange. Distances are measured in Å.

Table S1. Data Collection and Refinement Statistics for Set 2 NpG^o structures

Data Collection	ApG^o	TpG^o	CpG^o
Radiation Source	APS-24-IDE	APS-24-IDE	APS-24-IDE
Resolution (Å)	50-1.98	50–2.1	50-1.97
Unique reflections	30874	25999	32218
Completeness (%)[a]	99.9 (100.0)	99.9 (99.6)	99.9 (100.0)
Redundancy[a]	6.8 (6.9)	6.8 (6.5)	7.0 (7.1)
R_{merge} [a,b]	0.054 (0.479)	0.072 (0.652)	0.066 (0.487)
$< I / s >$ [a]	35.3 (3.3)	30.0 (3.1)	34.5 (4.7)
Space group	$P2_12_12_1$	$P2_12_12_1$	$P2_12_12_1$
Unit cell dimensions	a=45.21	a=45.50	a=45.27
	b=94.47	b=94.51	b=94.33
	c=103.85	c=103.61	c=103.80
Refinement and Model			
Resolution (Å)	32.7-1.98	32.7-1.80	32.7-1.70
R_{work} [a,c] (%)	20.1 (21.9)	18.8 (20.2)	17.9 (18.6)
R_{free} [a,c] (%)	23.3 (25.5)	22.3 (25.2)	20.7 (22.7)
Mean *B*-factors			
Protein	37.39	35.49	28.29
Water	43.39	41.64	42.34
R.m.s. deviation from ideality			
Bond lengths (Å)	0.004	0.005	0.004
Bond angles (°)	0.851	0.953	0.868
Ramachandran plot[d] (%)			
Most favored	93.9	95.3	94.4
Additionally allowed	5.6	3.8	5.2
Generously allowed	0.5	0.9	0.5
PDB ID	3U6Q	3U6M	3U6L

[a] Values in parenthesis refer to the highest resolution shell.

[b] $R_{merge} = \Sigma | I - < I > | / \Sigma < I >$; where I is the observed intensity.

[c] $R_{work} = \Sigma | F_o - F_c | / \Sigma | F_o |$; where F_o and F_c are the observed and calculated structure factor amplitudes, respectively.

R_{free} was calculated based on 5% data randomly selected and omitted throughout structure refinement (34).

[d] Values calculated using PROCHECK (31).

Figure S1

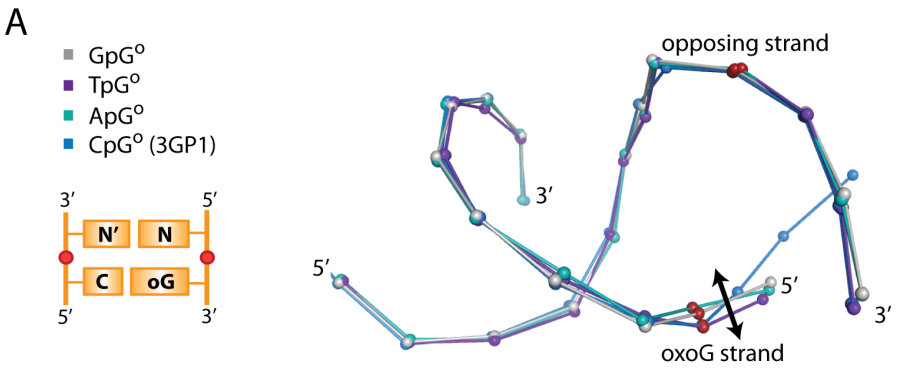
A
GpG°
TpG°
ApG°
CpG° (3GP1)
3′
5′
N′
N
C
oG
5′
3′
opposing strand
3′
5′
5′
3′
oxoG strand

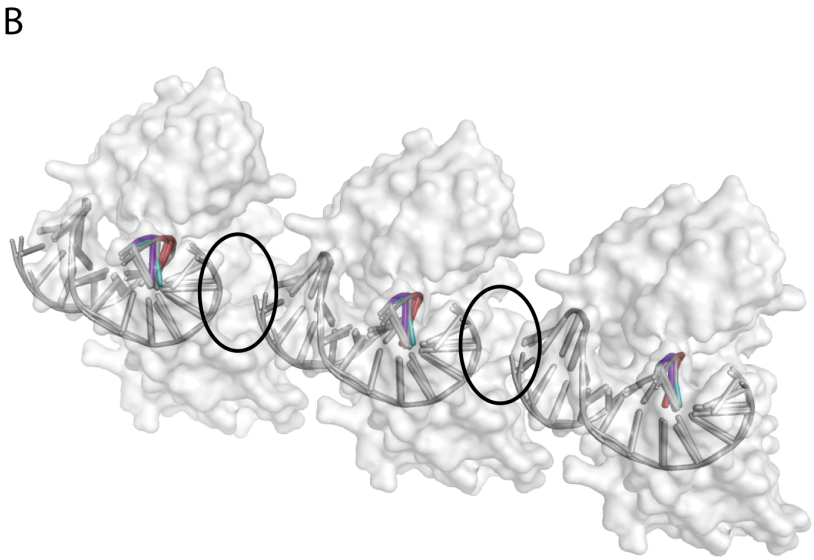
B

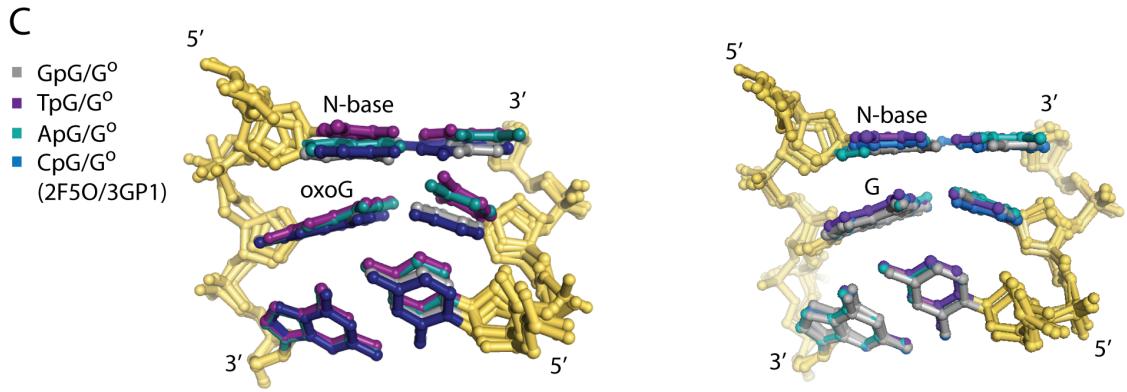
C
GpG/G°
TpG/G°
ApG/G°
CpG/G°
(2F5O/3GP1)
5′
N-base
3′
oxoG
3′
5′
5′
N-base
3′
G
3′
5′

Figure S2

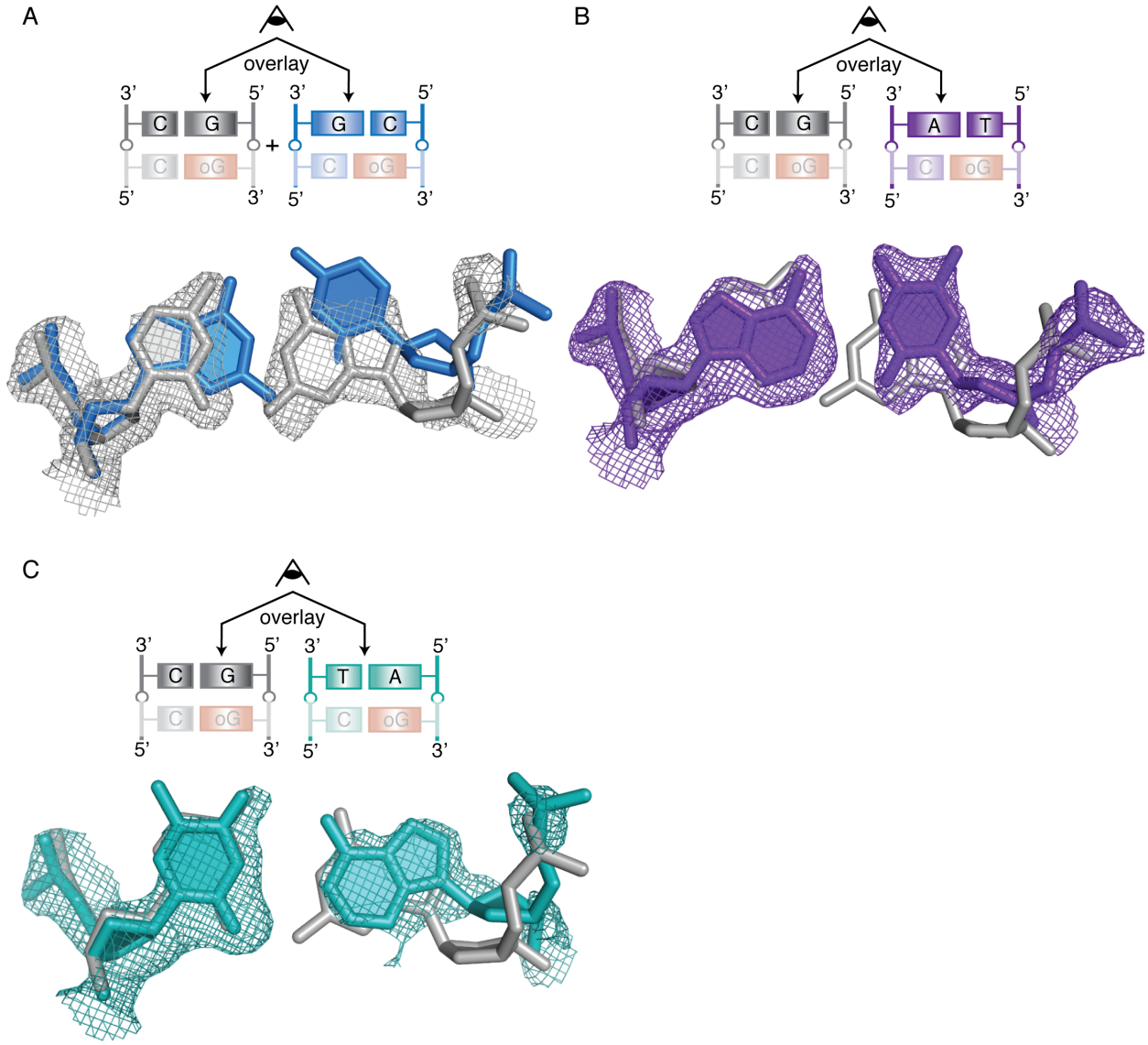

Figure S3

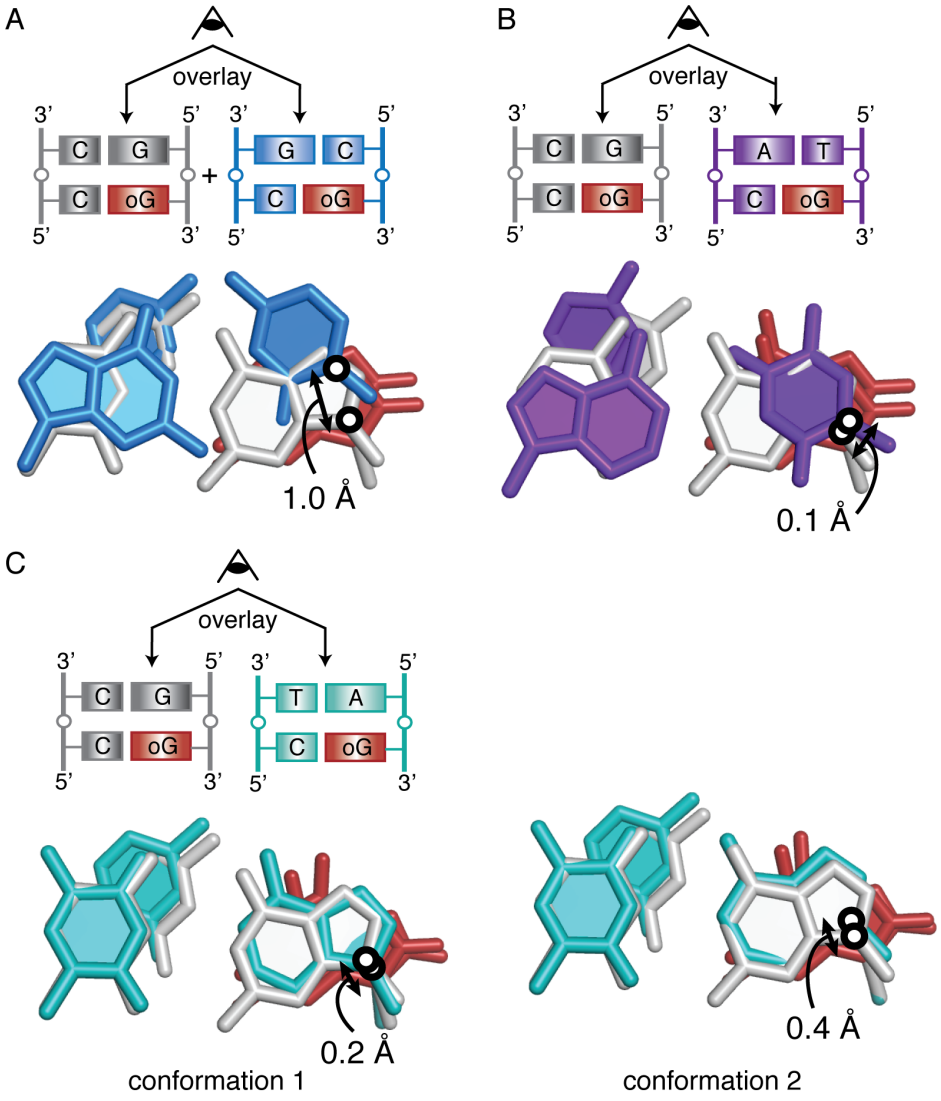
A
overlay
3'
5'
C
G
oG
1.0 Å
B
A
T
0.1 Å
C
T
A
0.2 Å
conformation 1
0.4 Å
conformation 2

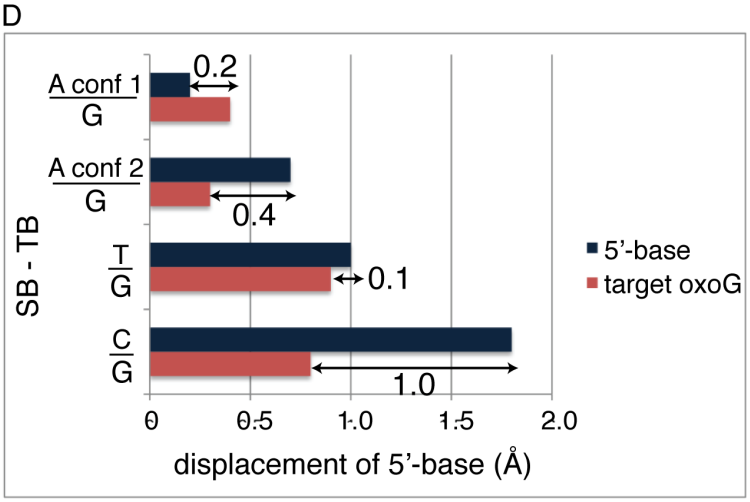
D
A conf 1
G
0.2
A conf 2
0.4
T
0.1
C
1.0
SB - TB
0
0.5
1.0
1.5
2.0
displacement of 5'-base (Å)
5'-base
target oxoG

Figure S4

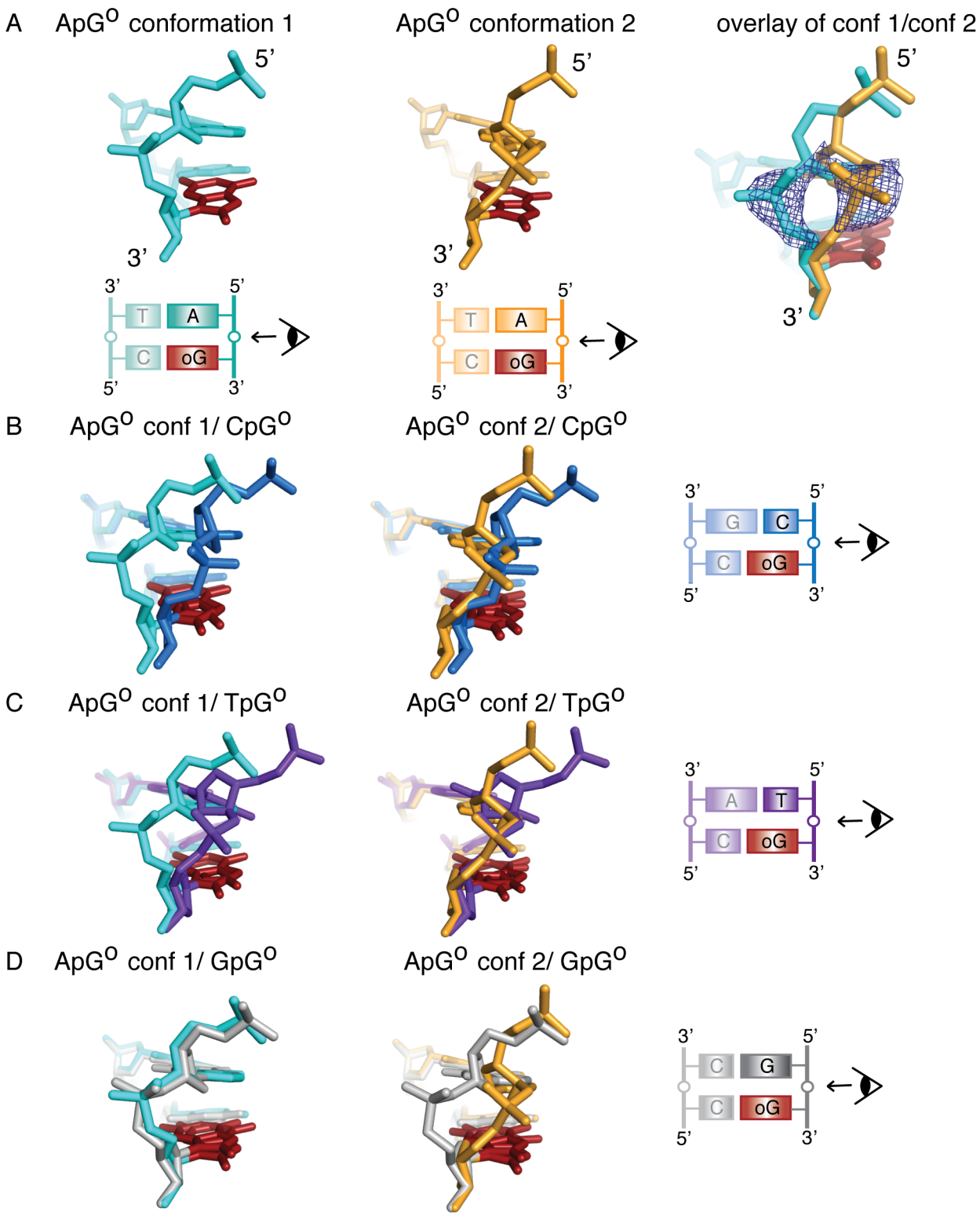
A
ApG^{O} conformation 1
ApG^{O} conformation 2
overlay of conf 1/conf 2
5'
3'
T
A
C
oG
B
ApG^{O} conf 1/ CpG^{O}
ApG^{O} conf 2/ CpG^{O}
G
C
C
Ap^{O} conf 1/ TpG^{O}
ApG^{O} conf 2/ TpG^{O}
A
T
C
oG
D
ApG^{O} conf 1/ GpG^{O}
ApG^{O} conf 2/ GpG^{O}
C
G
C
oG

Figure S5

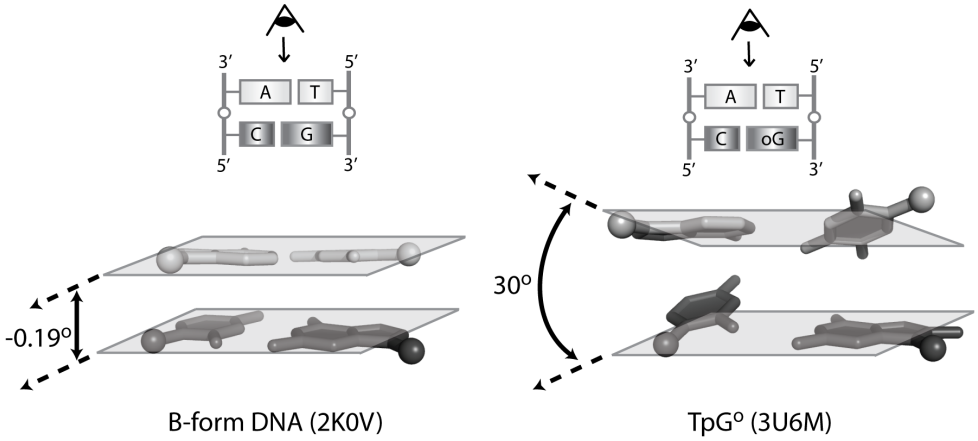

NpG/G°	Roll (°)
GpG°	11
CpG°	6.8
TpG°	30
ApG°	15

Figure S6

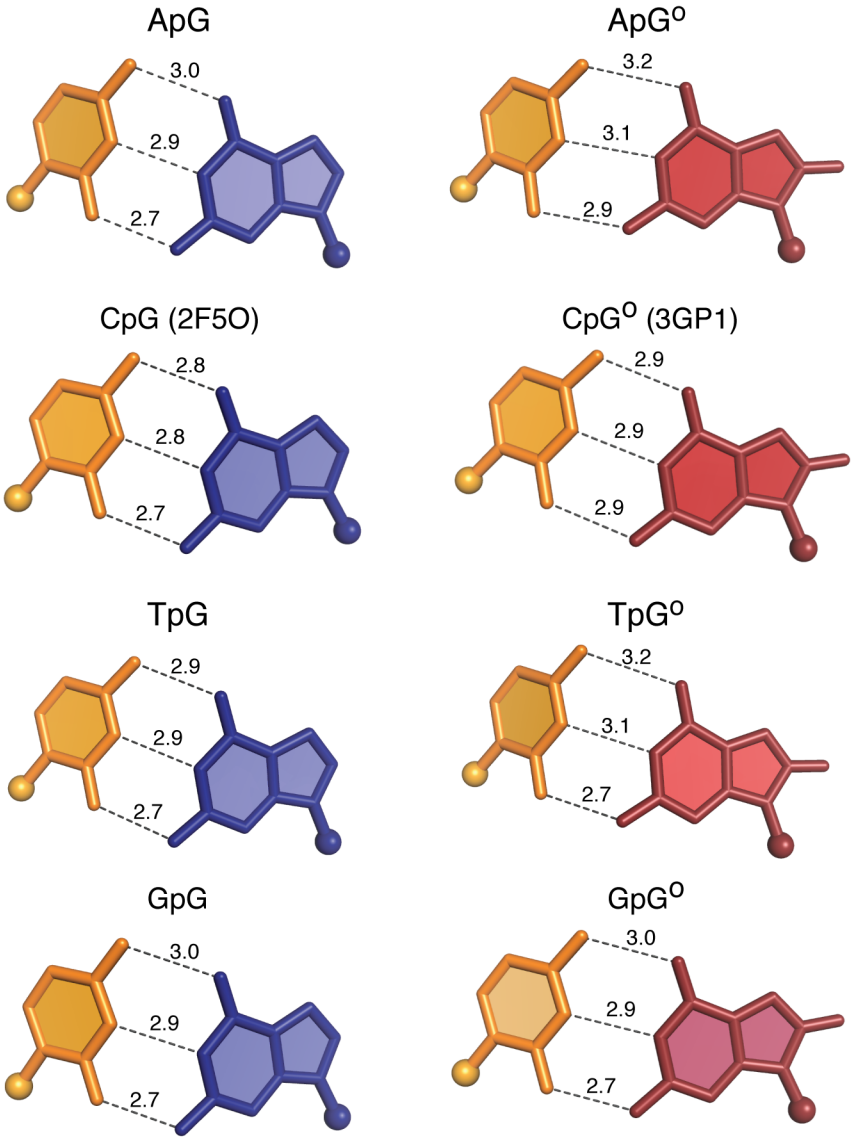
ApG
3.0
2.9
2.7
ApG^{O}
3.2
3.1
2.9
CpG (2F5O)
2.8
2.8
2.7
CpG^{O} (3GP1)
2.9
2.9
2.9
TpG
2.9
2.9
2.7
TpG^{O}
3.2
3.1
2.7
GpG
3.0
2.9
2.7
GpG^{O}
3.0
2.9
2.7